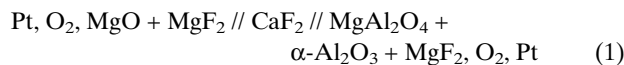


## Nanocrystalline MgAl<sub>2</sub>O<sub>4</sub>: Measurement of Thermodynamic Properties Using a Solid State Cell\*\*

By K. Thomas Jacob,\* Kampurath P. Jayadevan,  
Ram M. Mallya, and Yoshio Waseda

Most materials in their nanocrystalline state exhibit unusual properties. The tremendous enhancement of mechanical, physical, and chemical properties caused by the fine admixture of order (inside the crystallites) and disorder (in the grain boundary regions) is being exploited in a number of frontier technologies. A concern in the use of nanocrystalline materials is their stability during high temperature exposure, either while processing or in service. There is no experimental data in the literature on the Gibbs energy of formation of any nanocrystalline material and no standard technique is available for measurement, especially at elevated temperatures. Quantitative information on the thermodynamic driving force for degradation to the microcrystalline state and mechanistic understanding of the degradation processes would be useful in the design and processing of nanocrystalline materials for new applications. Reliable information on surface and interfacial properties of ceramic materials, which provide important guidelines for understanding nanocrystalline materials, are not available in the literature, even for model systems. Magnesium aluminate, which is used as an adsorbent for removing surfactants from aqueous solutions, as a support material for transition metal and lanthanide phosphors, and as a catalyst, was selected as a model compound in this study.

Reported in this communication is a novel application of the solid state electrochemical technique for probing the thermodynamic state of nanocrystalline MgAl<sub>2</sub>O<sub>4</sub> at high temperatures. The method has been used recently for the measurement of the Gibbs energy of microcrystalline MgAl<sub>2</sub>O<sub>4</sub>.<sup>[1]</sup> Although the principle of this method for thermodynamic measurements was outlined in the classic papers of Kiukkola and Wagner,<sup>[2,3]</sup> the technique has not been applied to nanocrystalline materials. The reversible electromotive force (emf) of the cell was measured as a function of temperature in the range 900 to 1250 K.



The cell is written such that the right-hand electrode is positive. Single crystal CaF<sub>2</sub> was used as the solid electrolyte and the cell was operated under dry oxygen. The reference electrode consisted of an intimate equimolar mixture of MgO and MgF<sub>2</sub> powders, compacted at a pressure of 250 MPa. Similarly, the working electrode was a compacted equimolar mixture of MgAl<sub>2</sub>O<sub>4</sub>,  $\alpha$ -Al<sub>2</sub>O<sub>3</sub>, and MgF<sub>2</sub>. The particle size of the powders used to prepare the reference and working electrodes usually vary from 2 to 10  $\mu\text{m}$ . In a recent study of the Gibbs energy of formation of MgAl<sub>2</sub>O<sub>4</sub>,<sup>[1]</sup> the average size of the aluminate particles used, as determined by scanning electron microscopy (SEM), was 3  $\mu\text{m}$ . In the present study, the measurements were made using nanocrystalline MgAl<sub>2</sub>O<sub>4</sub> powders, keeping all other conditions the same.

To obtain constant and reversible emf at any given temperature, it was necessary to remove moisture completely in the ceramic enclosure surrounding the cell. Formation of CaO on the surface of CaF<sub>2</sub>, by the reaction of water vapor with the solid electrolyte, was found to degrade the performance of the cell. The removal of water vapor adsorbed on ceramic materials was achieved by repeated evacuation to 10<sup>-4</sup> Pa and refilling with dry oxygen at high temperature before the start of each experiment. The reversibility of the cell was checked by microcoulometric titration (~ 50  $\mu\text{A}$  for 3 min) in both directions using an external potential source.

The nanocrystalline powders, made by coprecipitation of hydroxides, were subjected to controlled thermal processing and finally annealed at 1273 K for 10 h before use. The stoichiometry of the sample was confirmed by inductively coupled plasma atomic emission spectroscopy (ICPAES). Powder X-ray diffraction (XRD) analysis, transmission electron microscopy (TEM), Brunauer-Emmett-Teller (BET) analysis, and <sup>27</sup>Al magic angle spinning nuclear magnetic resonance (MASNMR) spectroscopy were used to characterize the powders. A typical XRD pattern is shown in Figure 1a. The average particle size of the powders was calculated from peak broadening using the Scherrer formula, after subtracting the contribution of background and Cu K $\alpha_2$  radiation from the observed diffraction profile. All well-defined peaks were used and an average value was calculated. Using the Williamson-Hall method<sup>[4]</sup> the absence of strain contribution to peak broadening was confirmed (Fig. 1b). TEM observations were compatible with the average particle size derived from XRD. The crystallites appear to be mainly cubic, with some in octahedral and dodecahedral forms.

The reversible emf of the cell is shown as a function of temperature for different particle sizes in Figure 2. The emf was generally reproducible on cycling temperature and unaffected by minor changes in the flow rate of oxygen gas over the electrodes. Nanoparticles tend to coarsen with time at high temperature. For example, the average particle

[\*] Prof. K. T. Jacob, Dr. K. P. Jayadevan  
Materials Research Centre and Department of Metallurgy  
Indian Institute of Science, Bangalore 560 012 (India)

Prof. R. M. Mallya  
Jawaharlal Nehru Centre for Advanced Scientific Research  
Jakkur, Bangalore 560 064 (India)

Prof. Y. Waseda  
Institute for Advanced Materials Processing  
Tohoku University, Sendai 980-8577 (Japan)

[\*\*] K. P. J. thanks the Council of Scientific and Industrial Research (C.S.I.R.), India, for financial assistance.

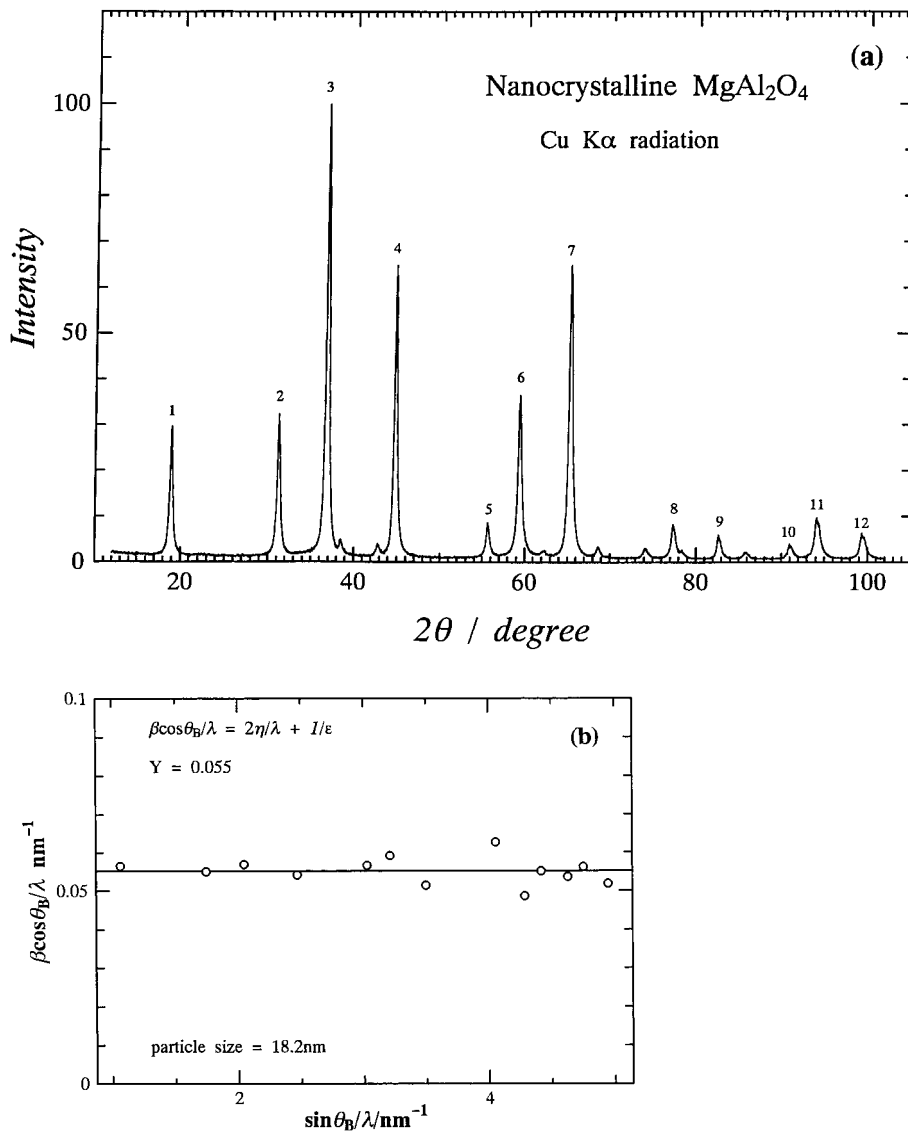
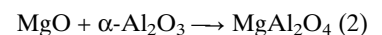


Fig. 1. a) XRD pattern of nanocrystalline  $\text{MgAl}_2\text{O}_4$  powder. b) Williamson-Hall analysis of peak broadening indicating the absence of strain;  $\beta$  represents the total line broadening and  $\varepsilon$  is the size of the crystallite.

size of  $\text{MgAl}_2\text{O}_4$  increases from 12 nm to 15 nm in 12 h at 1273 K. However, the coarsening rate is reduced by a factor of three when  $\text{MgAl}_2\text{O}_4$  is mixed with  $\alpha\text{-Al}_2\text{O}_3$  (2  $\mu\text{m}$ ) and  $\text{MgF}_2$  (5  $\mu\text{m}$ ) in equimolar amounts. Coarsening is much less pronounced for larger particles and at lower temperatures. During measurements on nanocrystalline  $\text{MgAl}_2\text{O}_4$  having a particle size of 18.2 nm, a small systematic drift in emf with time was detected at  $T > 1150$  K, attributable to particle coarsening. The magnitude of the drift at the highest temperature of measurement was  $-0.5 \text{ mV h}^{-1}$ . Hence, measurements at the higher temperatures were done with a new sample at each temperature. The emf corresponding to the particle size at the start (18.2 nm) was obtained by extrapolation of reversible emf to zero time. The corrections were relatively small. However, problems related to coarsening prevented measurements on smaller particles.

Within experimental error, emf varies linearly with temperature for each particle size. The results of regression analysis are summarized in Table 1. The maximum error ( $2\sigma$ ) in emf for the smallest particles is  $\pm 2$  mV. Both the value of the emf at a fixed temperature and the slope of the line changed systematically with the average particle size. There is a large decrease in emf with reduction in particle size in the nano range.

Since the oxygen pressure is the same over both the electrodes, the virtual cell reaction is:



The reactants  $\text{MgO}$  and  $\alpha\text{-Al}_2\text{O}_3$  are essentially in their pure standard states, since their particle sizes fall in the range 2 to 10  $\mu\text{m}$ . When the particle size of  $\text{MgAl}_2\text{O}_4$  is 3  $\mu\text{m}$ , the emf of the cell ( $E$ ) gives essentially the standard molar Gibbs energy of formation of  $\text{MgAl}_2\text{O}_4$  ( $\Delta G_f^\circ$ ) from its component oxides.<sup>[1]</sup> The emf of the cell with nanocrystalline aluminate material at the working electrode is a measure of the Gibbs energy of formation ( $\Delta G_f$ ) of nanocrystalline  $\text{MgAl}_2\text{O}_4$  from its component oxides in their normal thermodynamic reference states:

$$\Delta G_f = -2FE \quad (3)$$

where  $F$  is the Faraday constant. The corresponding enthalpy and entropy of formation of  $\text{MgAl}_2\text{O}_4$  for each particle size can be obtained from the temperature coefficient of emf:

$$\Delta H_f = -2FE + 2FT (dE/dT) \quad (4)$$

$$\Delta S_f = 2F (dE/dT) \quad (5)$$

The enthalpy and entropy of formation are average values in the temperature range of measurement. The high-temperature thermodynamic properties of  $\text{MgAl}_2\text{O}_4$  are plotted in Figure 3 as a function of its molar surface area ( $A$ ). Surface area is calculated from the mean particle size assuming cubic geometry. The calculated values agree with-

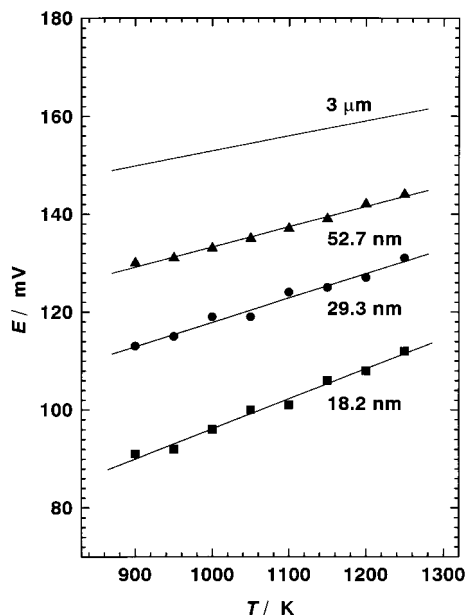


Fig. 2. Temperature dependence of the emf of the solid state cell for different particle sizes of  $\text{MgAl}_2\text{O}_4$ .

Table 1. Summary of experimental data.

$\text{MgAl}_2\text{O}_4$ particle size [nm]	$E$ [mV]	$\Delta G_f(\text{MgAl}_2\text{O}_4)$ [a] [J mol <sup>-1</sup> ]
18.2	$34.7 + 6.14 \times 10^{-2}T (\pm 2)$	$-6700 - 11.84T (\pm 390)$
29.3	$68.1 + 4.98 \times 10^{-2}T (\pm 2)$	$-13140 - 9.61T (\pm 390)$
52.7	$92.1 + 4.12 \times 10^{-2}T (\pm 1.1)$	$-17775 - 7.95T (\pm 220)$
3000	$122.3 + 3.06 \times 10^{-2}T (\pm 0.8)$ [1]	$-23600 - 5.91T (\pm 150)$ [1]

[a] Gibbs energy of formation of  $\text{MgAl}_2\text{O}_4$  from microcrystalline (5–10  $\mu\text{m}$ )  $\text{MgO}$  and  $\alpha\text{-Al}_2\text{O}_3$ .

in 4% with direct determination of the surface area by the BET technique on a few samples. The uncertainty limits are based on twice the standard error estimate ( $2\sigma$ ) for the emf. The thermodynamic properties increase linearly with surface area:

$$\Delta G_f(1200 \text{ K}) = -30740 + 0.7514A (\pm 300) \text{ J mol}^{-1} \quad (6)$$

$$\Delta H_f = -23690 + 1.299A (\pm 1300) \text{ J mol}^{-1} \quad (7)$$

$$\Delta S_f = 5.878 + 4.565 \times 10^{-4}A (\pm 1.1) \text{ J mol}^{-1} \text{ K}^{-1} \quad (8)$$

The values obtained by extrapolation to the zero surface area are the standard molar properties. The thermodynamic properties of  $\text{MgAl}_2\text{O}_4$  with particle size of 3  $\mu\text{m}$  are almost identical with the standard molar properties. This finding validates the established practice in our laboratories of using particles in the micrometer range for standard thermodynamic measurements, a practice not universally followed. A comparative discussion of the standard thermodynamic data on  $\text{MgAl}_2\text{O}_4$  obtained from our emf measurements has been presented earlier.<sup>[1]</sup>

The results obtained in this study indicate that nanocrystalline  $\text{MgAl}_2\text{O}_4$  below 13 nm ( $A = 18237 \text{ m}^2 \text{ mol}^{-1}$ ) has a

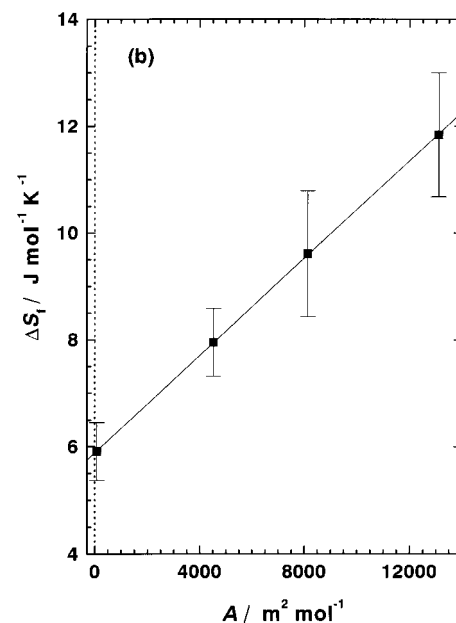
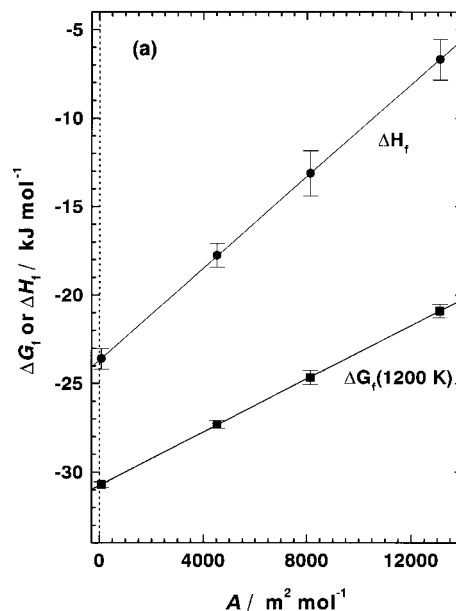


Fig. 3. a) Variation of the Gibbs energy and enthalpy of formation of  $\text{MgAl}_2\text{O}_4$ , from microcrystalline (2–10  $\mu\text{m}$ ) binary oxides  $\text{MgO}$  and  $\alpha\text{-Al}_2\text{O}_3$ , with molar surface area of  $\text{MgAl}_2\text{O}_4$ . b) Variation of the corresponding entropy of formation with surface area.

higher enthalpy relative to component oxides ( $\text{MgO}$  and  $\alpha\text{-Al}_2\text{O}_3$ ) in the microcrystalline form. Below 5.8 nm ( $A = 40910 \text{ m}^2 \text{ mol}^{-1}$ ) at 1200 K, the Gibbs energy of the spinel becomes higher than that of an equimolar mixture of microcrystalline component oxides. Smaller crystals can therefore be produced only via the solution route or starting with nanocrystalline binary oxides. The exact limits of stability can be deduced only when Gibbs energies of the binary oxides in the nanocrystalline form become available.

The surface excess properties can be derived from the slopes of the lines in Figure 3a and 3b. For example, from

the variation of the Gibbs energy of formation with surface area, the surface Gibbs energy is obtained as  $0.751 \text{ J m}^{-2}$  ( $\pm 0.025$ ) at 1200 K. The surface enthalpy is  $1.30 \text{ J m}^{-2}$  ( $\pm 0.08$ ) and the surface entropy is  $4.57 \times 10^{-4} \text{ J m}^{-2} \text{ K}^{-1}$  ( $\pm 0.75$ ) at a mean temperature of 1075 K. Both the surface enthalpy and entropy have the same sign. The two contributions partly compensate each other, producing a less pronounced increase in Gibbs energy with increasing temperature. McHale and coworkers<sup>[5]</sup> have recently obtained a value of  $1.8 \text{ J m}^{-2}$  ( $\pm 0.3$ ) for the surface energy (enthalpy) of  $\text{MgAl}_2\text{O}_4$  at room temperature from drop solution calorimetry in molten lead borate ( $2\text{PbO} \cdot \text{B}_2\text{O}_3$ ) at 975 K. The larger uncertainty in the calorimetric value is caused by two factors. First, the excess enthalpy of the nanocrystalline powder was obtained as a relatively small difference between larger enthalpies of solution of coarse and nano particles. Second, the nano particles at room temperature used in their experiment contained a substantial amount of adsorbed water, and approximate corrections had to be applied for heating and removal of this water. For the smallest particles, the error in the enthalpy of solution is  $\pm 7.3 \text{ kJ mol}^{-1}$ . In contrast, the Gibbs energy of formation is obtained directly with a much higher degree of accuracy of  $\pm 0.4 \text{ kJ mol}^{-1}$  by the emf method; the derived enthalpy is associated with an uncertainty of  $\pm 1.3 \text{ kJ mol}^{-1}$ . The improved precision obtained by the use of high-temperature solid-state galvanic cell techniques opens a new route for the study of the energetics of the nanocrystalline state.

A reduction in the MASNMR signal intensity with particle size was observed. Assuming that the amount of Al in a particular coordination is proportional to the area under the peak, the distribution of Al between the tetrahedral and octahedral sites was evaluated. Because of the lower intensity, the broadening of the Al(6) peak, and the positioning of Al(4) sideband on the tail of the Al(6) asymmetric peak, the cation distribution in nanocrystalline material cannot be obtained with sufficient accuracy. Nevertheless, for vacuum treated samples quenched from 1273 K, the cation disorder parameter ( $x$ ) increases from a value of 0.33 ( $\pm 0.02$ ) for  $3 \mu\text{m}$  powder to 0.35 ( $\pm 0.03$ ) for  $52.7 \text{ nm}$ , 0.37 ( $\pm 0.03$ ) for  $29.3 \text{ nm}$ , and 0.40 ( $\pm 0.04$ ) for  $18.2 \text{ nm}$  particles. The disorder parameter denotes the ionic fraction of Al on the tetrahedral site. This increase in cation disorder of nanocrystalline material is less pronounced than that reported by McHale and coworkers<sup>[5]</sup> ( $x = 0.59$ ). The presence of 0.72 mole of  $\text{H}_2\text{O}$  per mole of  $\text{MgAl}_2\text{O}_4$  and the poorly crystalline nature of the spinel are probably responsible for the higher apparent cation disorder in their sample. The loss of MASNMR signal intensity with increasing surface area has been observed in  $\gamma\text{-Al}_2\text{O}_3$ . According to O'Reilly<sup>[6]</sup> and Huggins and Ellis<sup>[7]</sup> the first two molecular layers of  $\text{Al}_2\text{O}_3$  do not contribute to the NMR signal. If this is also applicable to the spinel, then the MASNMR spectra show change in cation distribution in the bulk crystal. Only a fraction ( $1.2 \text{ J mol}^{-1} \text{ K}^{-1}$ ) of the observed increase in entropy of the nanocrystalline material

with an average particle size of  $18.2 \text{ nm}$  ( $5.97 \text{ J mol}^{-1} \text{ K}^{-1}$ ) is due to increase in cation disorder inside the crystal.<sup>[8]</sup> The major contribution is from change in coordination number and lattice vibrations in the surface region.

In this communication a new solid-state electrochemical method for the accurate determination of high-temperature surface thermodynamic properties of nanocrystalline ceramics is documented. The surface excess Gibbs energy of crystalline  $\text{MgAl}_2\text{O}_4$  at 1200 K is  $0.751 \text{ J m}^{-2}$  ( $\pm 0.025$ ). The corresponding surface enthalpy and entropy of  $\text{MgAl}_2\text{O}_4$  are  $1.30 \text{ J m}^{-2}$  ( $\pm 0.08$ ) and  $4.57 \times 10^{-4} \text{ J m}^{-2} \text{ K}^{-1}$  ( $\pm 0.75$ ), respectively. The lowest size limit is set by the kinetics of coarsening of the nanocrystalline material at the working electrode. With respect to the present technique, the particle growth is retarded by other microcrystalline phases present in the electrode. In oxides with significantly higher surface energies, coarsening rates may be more rapid, limiting the technique to larger particles and lower temperatures. The method demonstrated here opens a new avenue, where none existed,<sup>[9]</sup> for the measurement of the Gibbs energy of nanocrystalline ceramics at moderately high temperatures. Quantitative information on the energetics of the nanocrystalline state is important for understanding the evolution of microstructure and hierarchy of transition states. Syntheses of nanocrystalline oxides often produce crystal structures that are not thermodynamically stable. Cubic  $\text{BaTiO}_3$ ,<sup>[10]</sup> tetragonal  $\text{ZrO}_2$ ,<sup>[11]</sup> monoclinic  $\text{Y}_2\text{O}_3$ ,<sup>[12]</sup> and  $\gamma\text{-Al}_2\text{O}_3$ ,<sup>[13,14]</sup> are some examples of stabilization of metastable forms in the finely divided form. It is important to establish whether the stabilization is caused by the lower surface Gibbs energy of the metastable form relative to stable variety, as suggested by the molecular dynamics simulations of Blonski and Garofalini<sup>[15]</sup> on  $\alpha$  and  $\gamma\text{-Al}_2\text{O}_3$ . Application of the technique developed in this study may provide an answer to this fundamental question.

## Experimental

A solution route was adopted for the synthesis of nanocrystalline  $\text{MgAl}_2\text{O}_4$ . The nitrates,  $\text{Mg}(\text{NO}_3)_2 \cdot 6\text{H}_2\text{O}$ , and  $\text{Al}(\text{NO}_3)_3 \cdot \text{H}_2\text{O}$ , were mixed in the stoichiometric ratio and dissolved in a minimum amount of distilled water.  $\text{NH}_4\text{OH}$  was added with rapid stirring and a white gelatinous precipitate consisting of a mixture of hydroxides was formed. The pH was controlled in the range 8 to 9 by adding conc.  $\text{HNO}_3$ . Rapid and uniform stirring for 4 h prevented agglomeration and increased the homogeneity. The precipitate was filtered using a Whatman 41 filter paper and the white wet-gel was dried at 373 K for 12 h. The dried gel was thermally processed at 483 K for 2 h, 683 K for 4 h, 823 K for 15 h, 1073 K for 10 h, and 1273 K for 10 h. The sample was quenched to room temperature after each heat treatment for characterization purposes. All other experimental conditions are similar to those used earlier in the study of microcrystalline  $\text{MgAl}_2\text{O}_4$ .<sup>[11]</sup> The apparatus and procedure used for the emf measurements was similar to that described elsewhere.<sup>[16,17]</sup> The electrode pellets were made by cold compaction at 100 MPa, and partial sintering at 1250 K in prepurified oxygen to sufficient strength to withstand spring loading in the high temperature emf cell.

Received: January 11, 1999  
Final version: November 22, 1999

- [1] K. T. Jacob, K. P. Jayadevan, Y. Waseda, *J. Am. Ceram. Soc.* **1998**, *81*, 209.
- [2] K. Kiukkola, C. Wagner, *J. Electrochem. Soc.* **1957**, *104*, 308.

- 
- [3] K. Kiukkola, C. Wagner, *J. Electrochem. Soc.* **1957**, *104*, 379.
- [4] G. K. Williamson, W. H. Hall, *Acta Metall.* **1953**, *1*, 22.
- [5] J. M. McHale, A. Navrotsky, R. J. Kirkpatrick, *Chem. Mater.* **1998**, *10*, 1083.
- [6] D. E. O'Reilly, *Adv. Catal.* **1960**, *12*, 31.
- [7] B. A. Huggins, D. E. Ellis, *J. Am. Chem. Soc.* **1992**, *114*, 2098.
- [8] K. T. Jacob, C. B. Alcock, *Metall. Trans. B* **1975**, *6B*, 215.
- [9] A. W. Adamson, *Physical Chemistry of Surfaces*, Wiley, New York **1990**.
- [10] S. S. Flaschen, *J. Am. Chem. Soc.* **1955**, *77*, 6194.
- [11] R. C. Garvie, *J. Phys. Chem.* **1978**, *82*, 218.
- [12] G. Skandan, C. M. Foster, H. Frase, M. N. Ali, J. C. Parker, H. Hahn, *Nanostruct. Mater.* **1992**, *1*, 313.
- [13] G. P. Johnston, R. Muenchausen, D. M. Smith, W. Fahrenholtz, S. Foltyn, *J. Am. Ceram. Soc.* **1992**, *75*, 3293.
- [14] P. M. Kumar, P. Borse, V. K. Rohatgi, S. V. Bhoraskar, P. Singh, M. Sastry, *Mater. Chem. Phys.* **1994**, *36*, 354.
- [15] S. Blonski, S. H. Garofalini, *Surf. Sci.* **1993**, *295*, 263.
- [16] M. Allibert, C. Chatillon, K. T. Jacob, R. Lourtau, *J. Am. Ceram. Soc.* **1981**, *64*, 307.
- [17] K. T. Jacob, K. P. Abraham, S. Ramachandran, *Metall. Trans. B* **1990**, *21B*, 521.